CONTRAST MEDIA & MOLECULAR IMAGING

Received: 18 January 2011, Revised: 11 April 2011, Accepted: 18 April 2011, Published online in Wiley Online Library: 2011

(wileyonlinelibrary.com) DOI: 10.1002/cmmi.452

Deuteration of a molecular probe for DNP hyperpolarization – a new approach and validation for choline chloride

Hyla Allouche-Arnon[a,b], Mathilde H. Lerche[c], Magnus Karlsson[c], Robert E. Lenkinski[d] and Rachel Katz-Brull[a,b]*

The promising dynamic nuclear polarization (DNP) for hyperpolarized ^{13}C-MRI/MRS of real-time metabolism *in vivo* is challenged by the limited number of agents with the required physical and biological properties. The physical requirement of a liquid-state T_1 of tens of seconds is mostly found for ^{13}C-carbons in small molecules that have no direct protons attached, i.e. carbonyl, carboxyl and certain quaternary carbons. Unfortunately, such carbon positions do not exist in a large number of metabolic agents, and chemical shift dispersion often limits detection of their chemical evolution. We have previously shown that direct deuteration of protonated carbon positions significantly prolongs the ^{13}C T_1 in the liquid state and provides potential ^{13}C-labeled agents with differential chemical shift with respect to metabolism. The Choline Molecular Probe [1,1,2,2-D$_4$, 2-^{13}C]choline chloride (CMP2) has recently been introduced as a means of studying choline metabolism in a hyperpolarized state. Here, the biophysical properties of CMP2 were characterized and compared with those of [1-^{13}C]pyruvate to evaluate the impact of molecular probe deuteration. The CMP2 solid-state polarization build-up time constant (30 min) and polarization level (24%) were comparable to those of [1-^{13}C]pyruvate. Both compounds' liquid state T_1 increased with temperature. The high-field T_1 of CMP2 compared favorably with [1-^{13}C]pyruvate. Thus, a deuterated agent demonstrated physical properties comparable to a hyperpolarized compound of already proven value, whereas both showed chemical shift dispersion that allowed monitoring of their metabolism. It is expected that the use of deuterated carbon-13 positions as reporting hyperpolarized nuclei will substantially expand the library of agents for DNP-MR. Copyright © 2011 John Wiley & Sons, Ltd.

Keywords: deuterium; choline; magnetic resonance spectroscopy; dynamic nuclear polarization; hyperpolarization; pyruvate; spin-lattice relaxation; magnetic field; blood

1. INTRODUCTION

Significant attention has been given to the hyperpolarization technology of dynamic nuclear polarization (DNP) following reports on how to preserve the enhanced ^{13}C-NMR signal in a liquid state, and that this signal can be used to measure real-time metabolism in animals (1,2). This intriguing application of hyperpolarized MRI is, however, challenged by the limited number of molecular probes possessing the required physical and biological properties. Since the enhanced MR signal needed to study real-time metabolism is created in the solid state, it cannot be regenerated once the molecular probe has been liquefied and will disappear with the liquid state relaxation constant, T_1. This time dependence limits and governs the selection of molecular probes. In order to show value as a metabolic probe (i.e. being taken up in cells and metabolized), the T_1 needs to be long enough for the signal to survive sample handling time and allow the metabolic system in question to function. Such a long liquid state T_1 has been found for ^{13}C-carbons in small molecules that have no direct protons attached, i.e. carbonyl, carboxyl and certain quaternary carbons. In fact, to date, all of the useful *in vivo* molecular probes utilized in this technology have contained a nonprotonated carbon 13-enriched positions, as in pyruvate (2), fumarate (3), *t*-butanol (4), acetate (5), fructose (6), acetic anhydride (7) and *α*-ketoisocaproic acid (8). Unfortunately, chemical shift dispersion is often limited for molecular probes that are ^{13}C-labeled in carbonyl and carboxyl carbons, hampering the detection of their metabolic products owing to chemical shift overlap. This has greatly limited the selection of molecular probes for this technology.

The Choline Molecular Probe [1,1,2,2-D$_4$, 2-^{13}C]choline chloride (CMP2) has recently been introduced as a means of studying choline metabolism in a DNP-driven hyperpolarized state (9). This choline analog was specifically designed to follow the metabolism

* *Correspondence to: R. Katz-Brull, Department of Radiology, Hadassah-Hebrew University Medical Center, Jerusalem, Israel.*
E-mail: rkb@hadassah.org.il

a *H. Allouche-Arnon, R. Katz-Brull*
Department of Radiology, Hadassah-Hebrew University Medical Center, Jerusalem, Israel

b *H. Allouche-Arnon, R. Katz-Brull*
BrainWatch Ltd, 27 Habarzel St, Tel-Aviv, Israel

c *M. H. Lerche, M. Karlsson*
Albeda Research, Gamle Carlsberg Vej 10, 2500 Valby, Denmark

d *R. E. Lenkinski*
Department of Radiology, Beth Israel Deaconess Medical Center and Harvard Medical School, Boston, Massachusetts, USA

of choline to acetylcholine owing to the unique chemical shift of the labeled carbon position (methylene 2), which provides an unequivocal signal of acetylcholine (9,10). The use of carbon-13 positions that are normally protonated for DNP hyperpolarization was first introduced with this molecular probe and provides a means of dramatically expanding the library of probes that may be used in combination with the DNP hyperpolarization technique. Because the CMP2 probe presents a new approach for designing molecular probes for DNP hyperpolarization, using a deuterated carbon-13 position as the active part of the molecule, we felt that it was important to investigate the performance of such an approach with respect to existing knowledge in the field. The most investigated hyperpolarized molecular probe to date is by far [1-^{13}C]pyruvate (pyruvate) with several papers describing investigations of its performance in cultured cells and tissues, and in solution (e.g. 11–13), and more than 20 papers describing *in vivo* applications (14,15). The pyruvate probe has excellent physical properties (relatively long T_1, high polarization, and fast polarization build-up). For these reasons, the pyruvate molecular probe is considered a 'gold standard' in the field.

In the current study we investigated the biophysical properties of the CMP2 probe and compared them with those of the [1-^{13}C]pyruvate probe. These included studies on T_1 and heteronuclear interactions as well as testing the probes in whole blood for signal decay. On the basis of the findings and understanding of the physical properties of the CMP2 molecular probe, the general concept of deuteration is evaluated.

2. RESULTS

The comparison and characterization of the probes' performance are described according to the steps involved in the preparation and the use of the hyperpolarized molecular probes *in vivo*, i.e. solid-state polarization, dissolution, T_1 in solution, effects of magnetic field and temperature and decay in blood. Considerations of heteronuclear decoupling are also presented.

2.1. Solid-state polarization

A DNP polarization protocol for CMP2 was developed and yielded a polarization build-up constant of 30 ± 2 min ($n = 4$), meaning that 95% of the polarization was achieved within 1.5 h. This polarization time (1.5 h) was found to be in the same order of magnitude as that of pyruvate (~1 h), which showed a build-up time constant of 18 ± 1 min ($n = 3$) in the same polarizer, operating at 3.35 T and ca. 1.3 K (see the Experimental section).

The polarization level reached 24 ± 8% ($n = 4$), which was comparable with the polarization of pyruvate (28 ± 1%, $n = 3$) in the same polarizer. These polarization levels were measured in liquid state, ca. 20 s after dissolution, at 14.1 and 9.4 T, respectively. We note that both the polarization level and the build-up time constant for CMP2 may be further improved when the polarization preparation is further optimized.

2.2. T_1 in liquid state – field dependence

It was previously shown that the T_1 of hyperpolarized compounds (lactate) can be critically dependent on the magnetic field (16). Here, we found a similar effect for pyruvate (Fig. 1). At 37 °C, the pyruvate T_1 (carbonyl carbon) was found to be significantly longer at a lower field strength (from ca. 34 s at 14.1 T to 70 s at 2.4 T, a clinically relevant field strength). The dependence of the T_1 of CMP2 on the magnetic field was investigated at 37 °C as well, at the ultra high fields of 7, 9.4, 11.8 and 14.1 T and at the fringe field of the latter (~5 gauss, low-field). The results are summarized in Fig. 1: the liquid state T_1 of CMP2 was found to be 13 s longer than that of pyruvate at 14.1 T and 37 °C. At 7 T and 9.4 T the T_1 of CMP2 (60 and 54 s, respectively) appeared comparable to that of pyruvate. The low-field T_1 of CMP2 was estimated by placing the enhanced sample in the fringe field of the unshielded 14.1 T magnet ($n = 1$) for intervals of 1 min. From this experiment it was concluded that the low-field T_1 is long (> 50 s). We note that, in this low-field study, the temperature was not well controlled and we expect the relevant temperature to be less than 37 °C, although that was the spectrometer probe's temperature. In Fig. 1, the dashed line connecting this low-field measurement to the other measurements represents this uncertainty in temperature, which may affect the T_1 as described below.

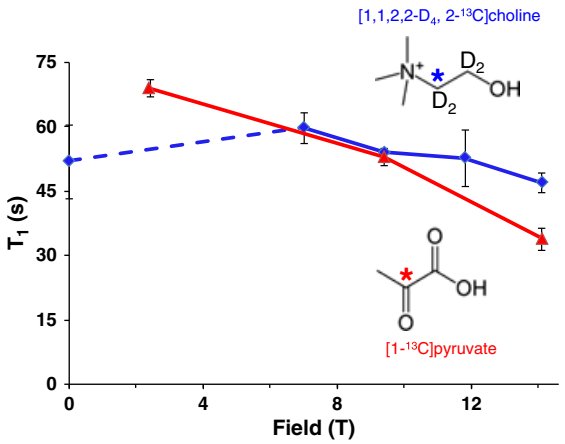

Figure 1. The T_1 of the carbon-13 position in the CMP2 (blue) and the pyruvate (red) molecular probes at various magnetic field strengths at 37 °C. The dashed line connecting the low-field measurement (~5 Gauss, fringe field of a 14.1 T spectrometer) to the 7 T measurement represents the uncertainty in the low-field measurement owing to a possible decrease in temperature leading to a lower T_1.

2.3. T_1 in liquid state – temperature dependence

Next, the effect of temperature on the T_1 in solution was investigated for both compounds. For pyruvate this effect was investigated at 9.4 T in the hyperpolarized state. For CMP2 this effect was investigated at 11.8 T under thermal equilibrium conditions, and at 14.1 T in a hyperpolarized state. The results are summarized in Table 1. Both probes appear to show a longer T_1 at higher temperatures and this effect appears to reproduce at the three different field strengths used here. The effect of temperature on T_1 was systematically investigated for the CMP2 probe. This investigation was carried out at thermal equilibrium conditions where the temperature can be carefully controlled. Indeed, the T_1 of CMP2 was found to be longer at higher temperatures. This finding clearly indicates that it would be favorable for both CMP2 and pyruvate hyperpolarized media to be maintained at above 37 °C prior to administration to the animal or subject, as opposed to the more practical option of handling and transporting the hyperpolarized media at room temperature.

Table 1. Dependence of T_1 on temperature

	18 °C	25 °C	37 °C	45 °C	41 °C
T_1 of CMP2 at 14.1 T (s)[a]	—	—	47 ± 2	56 ± 5	
T_1 of CMP2 at 11.8 T (s)[b]	35 ± 1	46 ± 6	53 ± 7	55 ± 5	
T_1 of pyruvate at 9.4 T (s)[c]	—	—	53 ± 2		60 ± 2

—, Not measured.
[a]Mean T_1 of the hyperpolarized decay curve. The error represents the standard deviation of the measurements: $n = 5$ at 37 °C, and $n = 3$ at 45 °C. For the latter, the temperature of the hyperpolarized state in this study was estimated to decrease from 50 to 40 °C within the measurement duration and is therefore reported as 45 °C.
[b]The T_1 at thermal equilibrium conditions. The error represents the confidence interval of the inversion recovery curve fit for each point ($n = 1$).
[c]Mean T_1 of the hyperpolarized decay curve. The error represents the standard deviation of the measurements ($n = 3$).

2.4. T_1 in liquid state – decay in blood

The next step in the hyperpolarized media path is the transportation of the molecular probe to the target area via the blood circulation, following an intravenous administration. During this time, the polarization decays according to the added possible effects of magnetic field, temperature and the micro- and macro-environment of the blood. For this reason, the effect of whole blood on the T_1 of both probes was investigated. To comparatively study this effect, CMP2 and pyruvate were polarized simultaneously in the same sample. This was achieved by creating glassy beads of the polarization preparation of each and loading both beads into the same DNP sample holder. The sample was polarized, dissolved (in pyruvate dissolution buffer) and mixed with whole blood as described in the Experimental section. Then, the decay curves of both compounds were recorded simultaneously in the same spectra. Figure 2 demonstrates a typical study, showing the decay of CMP2 and pyruvate, but also the build-up of the hyperpolarized lactate signal in the blood. The whole-blood decay time constant (T_{decay}) of the polarized state was 39 ± 2 s ($n = 3$) for CMP2 and 23 ± 2 s ($n = 3$) for pyruvate at 14.1 T and 37 °C. The term T_{decay} is used here to also accommodate the decay of the signal owing to (unwanted) exchange and metabolism to lactate.

Lactate signal build-up was observed in the spectra within a few seconds after the addition of the hyperpolarized media (containing 19.5 mM pyruvate) to the blood (Fig. 2). In contrast, CMP2 was not metabolized or exchanged in the blood and a single signal was observed throughout the study. Because CMP2 did not metabolize/exchange in blood and its T_1 appeared relatively insensitive to the magnetic field, we did not further investigate its T_{decay} at other magnetic fields and concluded that 39 ± 2 s represents a lower limit for its T_{decay} in blood for various *in vivo* applications. However, the T_1 of pyruvate appeared to be dependent on the magnetic field and therefore we have characterized its T_{decay} in blood with respect to the magnetic field. The T_{decay} of pyruvate at 37 °C in whole blood was found to be 23 ± 2 s ($n = 3$), 32 ± 3 s ($n = 3$), and 37 ± 8 s ($n = 3$), at 14.1, 9.4 and 2.4 T, respectively.

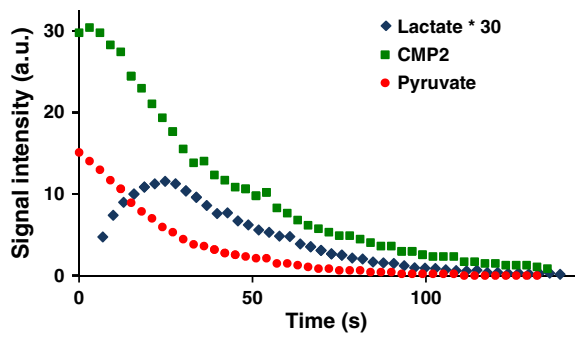

Figure 2. A typical T_{decay} curve for CMP2 and pyruvate in whole blood at 14.1 T. The build-up of lactate signal in the blood is clearly seen. The lactate signal intensity was augmented 30-fold for clarity.

2.5. Deuterium decoupling

Deuterium decoupling of CMP2 was performed at 11.8 T at thermal equilibrium. The deuterium split was eliminated as expected and the gain in the signal-to-noise ratio (SNR) of the main signal was 3.1, in agreement with the expected 3-fold theoretical gain (Fig. 3).

Next we investigated whether deuterium decoupling is also feasible for a metabolic product of CMP2, namely [1,1,2,2-D_4, 2-^{13}C]acetylcholine (AcCMP2). A mixture of CMP2 and AcCMP2 was obtained by the enzymatic acetyltransferase reaction on CMP2 as described in the Experimental section. As expected, as a result of deuterium decoupling, the deuterium split was eliminated from both CMP2 and AcCMP2 signals and the chemical shift resolution between the signals increased appropriately (Fig. 3).

2.6. Proton decoupling

The quaternary methyl protons were irradiated (as the rest of the molecule is deuterated), resulting in an increase in the SNR of the carbon-13 signal of CMP2. Figure 4 shows an increase of 1.9-fold in SNR when proton irradiation was applied during the acquisition (proton decoupling) and a total increase of 2.2 when proton irradiation was also applied prior to the acquisition (nuclear Overhauser effect and proton decoupling). Irradiation during the acquisition appeared to reduce the signal width owing to removal of long-range couplings and split, and thus led to an increase in the signal amplitude (Fig. 4B).

In principle, the nuclear Overhauser effect is likely to be inadvertent to the carbon-13 hyperpolarized signal owing to polarization transfer from ^{13}C to ^{1}H, which may reduce the ^{13}C hyperpolarized signal intensity. However, proton decoupling alone is not likely to have this effect and from the results shown here it appears that proton decoupling may offer an SNR advantage for hyperpolarized studies of CMP2.

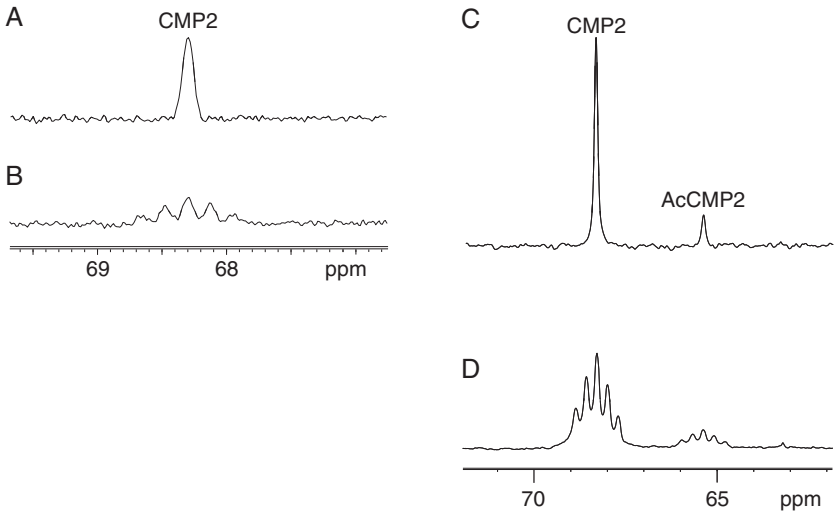

Figure 3. Deuterium decoupling of CMP2 and its acetylcholine metabolite. (A, B) Direct ^{13}C spectra of CMP2 (106 mM in water and 10% D_2O) at 11.8 T, acquired with and without deuterium decoupling, respectively. Each spectrum is an average of four transients. The elimination of the splitting from the signals is clearly visible in the deuterium decoupled spectrum (A) compared with the nondecoupled spectrum (B). (C, D) Direct ^{13}C spectra of a mixture of CMP2 and its acetylcholine metabolite (AcCMP2), which was obtained using an acetyltransferase reaction on CMP2 (as described in the Experimental section). The spectra were acquired with and without deuterium decoupling at 11.8 and 7 T, averaging 64 and 2300 transients, respectively. Because the spectra were recorded on two different spectrometers and with a time lag that could allow the acetyltransfrerase reaction to progress either way, a quantitative comparison between these two spectra (C and D) is not relevant.

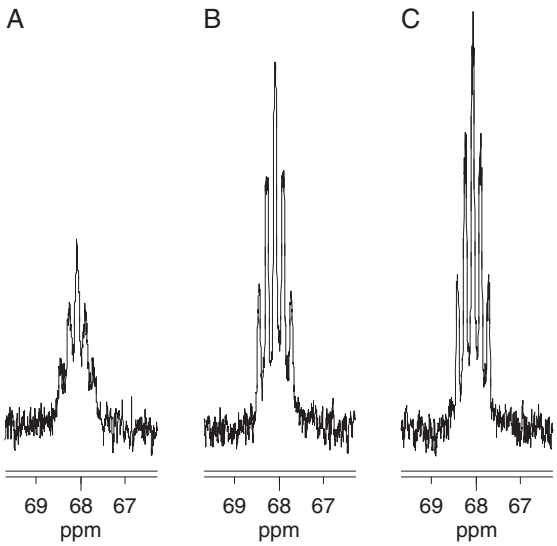

Figure 4. Proton decoupling for CMP2. The multiplet ^{13}C signal of CMP2 (106 mM in water and 10% D_2O) at 11.8 T is shown without any proton irradiation (A), in the presence of proton irradiation during acquisition (B, proton decoupling), and in the presence of proton irradiation throughout the measurement (C, nuclear Overhauser effect and decoupling).

3. DISCUSSION

We present an investigation into the properties of a DNP molecular agent that consists of a carbon-13 reporting nucleus directly bonded to two deuterium atoms and adjacent to two others. The effect of deuteration on adjacent carbon-13 positions' T_1 had been described before (17,18), and the deuteration strategy for the purpose of elongation of adjacent (but not directly bonded) hyperpolarized carbon-13 positions had been previously implemented with regard to *para*-hydrogen induced polarization (19–21). However, to the best of our knowledge the effects of deuteration on directly bonded carbon-13 positions that are used as reporting nuclei in the hyperpolarized DNP-MR technology have not been described before. An important aspect that results from this work is that deuteration of the reporting ^{13}C position does not impede the polarization build-up process, as manifested by a build-up time constant and level that are comparable to those of pyruvate – a well established DNP molecular agent.

It is noted that deuterated carbon-13 positions used as hyperpolarized reporting nuclei present a multi-line signal owing to the *J*-coupling with deuterium. In the case of one directly bonded deuterium the signal is split into three (with a 1:1:1 intensity ratio). In the case of two directly bonded deuterium nuclei, the signal is split into five with an intensity ratio of 1:2:3:2:1. In order to recover the loss of signal intensity and sharpen the resolution in the chemical shift dimension, deuterium decoupling may be applied. The theoretical gain in the signal intensity for the center signal would be 3-fold, both for one and two directly bonded deuterium nuclei. However, if other deuterium couplings exist, the increase in SNR owing to deuterium decoupling may even be higher. We have shown here that the SNR gain owing to deuterium decoupling in the CMP2 molecule is 3.1-fold.

In addition, the resolution between CMP2 and its acetylcholine product (AcCMP2) was improved by deuterium decoupling, by increasing the actual separation between the two signals in the chemical shift dimension. Therefore, it appears likely that the effects of deuterium decoupling (i.e. increase in SNR and

resolution) will be obtained for other metabolites of CMP2 as well. We conclude that deuterium decoupling for deuterated carbon-13 reporting nuclei and their metabolites solves two problems related to such positions: it improves the spectral resolution and recovers the signal intensity lost due to scalar coupling. Owing to the short time of irradiation needed for deuterium decoupling (the ^{13}C acquisition time), this approach is not expected to be limited by specific absorption rate requirements but this aspect requires further investigation.

The motivation for choosing the choline molecule as a target for this investigation was due to its positioning at the crossroads of essential metabolic processes (22): acetylation for the production of the neurotransmitter acetylcholine, phosphorylation for the production of phosphocholine and further to phospholipid metabolism, and oxidation to betaine and further to methylation reactions in the cell. In the same manner, pyruvate is at the crossroads of several major metabolic pathways, including the citric acid cycle, alanine metabolism and lactate production. In pyruvate, labeling of position 1 with ^{13}C as the reporting hyperpolarized nucleus allows monitoring of its metabolism to lactate, alanine, and bicarbonate (23). In choline, labeling of position 2 with ^{13}C (as in CMP2) allows monitoring of acetylcholine synthesis with a chemical shift difference of 2.9 ppm from choline (9). However, this position has only 0.9 and 1.3 ppm chemical shift difference from phosphocholine and betaine, respectively (9). To better resolve hyperpolarized phosphocholine and betaine, it is possible to label position 1 ([1,1,2,2-D_4,1-^{13}C]choline chloride, CMP1), which has a chemical shift difference of 2.4 and 113.7 ppm, respectively (9). The focus in the current study on CMP2 and not on CMP1 was predominantly due to its availability through the donation of this custom synthesized molecule. Nevertheless, position 1 is very similar to position 2 in terms of being directly bonded to 2 deuterium atoms and being adjacent to another two deuterons. Also, a previous investigation of deuteration of this position showed a similar T_1 elongation effect to that of position 2 (9). Previous studies showed that the deuterated methyl ^{13}Cs (9) and a nitrogen-15 nucleus (13,24,25) in the choline molecule show a long T_1 as well; however, the chemical shift differences to choline metabolites were too small to enable direct metabolic monitoring and were therefore excluded from the current study.

The investigation of T_1 dependence on field strength showed that the T_1 of the deuterated methylene carbon in CMP2 was less affected by field strength than pyruvate. We attribute this difference between CMP2 and pyruvate to the lower chemical shift anisotropy in the former as the electron distribution is generally more uniform in tetrahedral positions compared with carbonyl positions. This is a general concept relating not only to CMP2 but also to many compounds which would benefit from deuteration. As most DNP reporting nuclei today are placed in carbonyl positions (2,3,8), the direct deuteration approach is likely to substantially increase the portfolio of imaging agents and reporting nuclei within them that are useful for the DNP technology. For example, amino acids are examples of compounds that would be expected to benefit from deuteration because the chemical shift differences from the expected metabolites are often negligible when labeled in the carboxyl group position (or nonexistent in reactions of decarboxylation). In addition, the deuteration approach may provide a new strategy for designing imaging agents with longer T_1, especially when used at high fields.

The investigation of the T_{decay} of CMP2 and the T_{decay} of pyruvate in whole blood demonstrated that both are shortened by the blood environment. However, the percentage shortening was much greater for pyruvate (32% at 14.1 T). We attribute this effect to the combination of label exchange, metabolism to lactate in erythrocytes, and to blood protein binding. Indeed, a build-up of label in lactate was observed here, in agreement with previous reports in which it was attributed to exchange with the labeled hyperpolarized pyruvate pool and metabolism (26,27). The T_{decay} of CMP2 in whole blood was therefore significantly longer than that of pyruvate in the ultra high field of 14.1 T. Based on the entire set of investigations described herein, we predict that CMP2 T_{decay} will be longer or comparable to that of pyruvate at field strengths of 9.4 T and lower.

An important feature for the design of a metabolic molecular agent is its ability to cross cellular membranes and the rate constants of this process. *In vivo* studies, showing intracellular metabolism, as in the case of pyruvate, provide the most definite proof for a sufficiently rapid uptake process for hyperpolarized studies. Although this is yet to be demonstrated for choline, we briefly review here previous literature on choline transport in an attempt to predict the utility of the choline probe on *in vivo* hyperpolarized MR studies. In the brain, a specialized choline transporter is expressed on the blood–brain barrier cells, with a K_m of 39–42 μM and a V_{max} of up to 3.1 nmol/min/g (28). In the kidney an uptake mechanism with a K_m of 80–155 μM and a V_{max} of 71 pmol/μl water cell/min has been reported (29). Assuming that the kidney contains approximately 85% water, this rate can be expressed as 61 nmol/min/g. In rat liver cells, an uptake mechanism with a K_m of 340 μM and a V_{max} of 0.45 nmol/mg protein/15 s had been reported (30). Using a previously determined conversion factor of 21 mg protein/g tissue (31), the choline uptake V_{max} in the liver can be expressed as 38 nmol/min/g. In addition, previous studies of choline transport in breast cancer cells (32) and prostate cancer cells (33) showed a K_m of 20 and 6–9 μM, respectively, and a V_{max} of 20 nmol/mg protein/h and 1.7 nmol/mg protein/10 min, respectively. Using a conversion factor of 35 mg protein/g cell (34), these V_{max} values can be expressed as 12 and 6 nmol/min/g, respectively. The range of K_m values described here was attributed to the presence of high, intermediate, and low affinity choline transporters in various tissues (35). From these representative studies, it would appear that, under a physiological concentration of choline in the blood of 10–100 μM and at the high doses used in hyperpolarized studies of more than 10 μmol/kg, the kidney would be the main organ for choline uptake.

The level of choline taken up by the above tissues is expected to range between 3 and 55 nmol/min/g (or μM/min), considering a dose of 1 mg/kg CMP2. It is expected that this level of choline and its metabolites would be amenable to monitoring by hyperpolarized MR, considering that carbon-13 substrates at millimolar levels can be monitored using conventional spectroscopy and that hyperpolarization offers about four orders of magnitude increase in signal, although signal averaging considerations are different in hyperpolarized spectroscopy.

In principle, substitution of proton with a deuteron can lead to a significant isotopic effect on a molecular agent's pharmacological properties (36). However, we have previously shown that the substitution of the protons with deuterons at the methylenic positions did not affect the specific enzymatic conversion of choline to acetylcholine (9). It remains to be seen whether this substitution would lead to changes in the rates

of choline transport in various tissues, or in other choline metabolic pathways.

4. CONCLUSION

CMP2, a molecular probe in which the reporting ^{13}C nucleus is positioned in an sp3 carbon position and directly bonded to two deuterium atoms, compares favorably in several aspects to pyruvate, which is today's 'gold-standard' for DNP hyperpolarized molecular probes in which the reporting ^{13}C nucleus is in an sp2 position. These aspects include an apparent relative insensitivity of T_1 to magnetic field, longer T_{decay} in blood in ultra high magnetic fields, and lack of metabolism or label exchange in blood. In other aspects CMP2 is comparable to pyruvate and well suited as a biomedical DNP compound. It is predicted to polarize similarly fast and to a comparable high polarization as pyruvate. However, the ability of pyruvate to show metabolism *in vivo* has already been proven, while such ability is yet to be demonstrated with CMP2. Deuterium decoupling of CMP2 and its metabolites is likely to increase both the SNR and the resolution of CMP2 and its metabolites *in vivo*.

5. EXPERIMENTAL

5.1. Materials

[1,1,2,2-D_4,2-^{13}C]choline chloride was donated by BrainWatch Ltd (BW-42, BrainWatch Ltd, Tel-Aviv, Israel). The spectral characteristics of [1,1,2,2-D_4,2-^{13}C]choline chloride were: ^{13}C spectrum – singlet at 55.5 ppm, methyls at natural abundance; multiplet (1:2:3:2:1) at 68.3 ppm, each spilt to three (1:1:1), $J_{C\text{-}D} = 22.07$ Hz, $J_{C\text{-}14N} = 2.7$ Hz, N-$^{13}CD_2$-; ^1H spectrum – singlet at 3.2 ppm, methyls; ^2H spectrum – doublet at 3.33 ppm, $J_{C\text{-}D} = 22.07$ Hz, -N-$^{13}CD_2$-, singlet at 3.88 ppm, -CD_2-OH, as previously described (9). [1-^{13}C] pyruvate was obtained from Sigma-Aldrich (Copenhagen, Denmark). Trityl radical OX063, was obtained from GE Healthcare (London, UK). ProHance was purchased from Bracco Diagnostics Inc. (Italy). Carnitine acetyltransferase from pigeon breast muscle (EC 2.3.1.7) was obtained from Sigma-Aldrich (Rehovot, Israel). Acetyl CoA was obtained from Sigma-Aldrich (Rehovot, Israel).

5.2. NMR spectrometers

Several spectrometers located at various institutions were utilized in this study. High-resolution spectrometers included: an 11.8 T spectrometer (Varian, Palo Alto, CA) with a 5 mm direct multinuclei probe located at Hadassah-Hebrew University Medical Center, Israel; an 11.8 T spectrometer (Bruker, Germany) equipped with a cryo probe and a 5 mm direct multinuclei probe located at the Weizmann Institute of Science, Israel, which was used only for deuterium decoupling; a 14.1 T spectrometer (Bruker, Germany) with a 5 mm inverse detection and a 10 mm broad-band probe at Albeda Research, Denmark; and a 9.4 T spectrometer (Bruker, Germany) equipped with a 5 mm direct multinuclei probe located at Albeda Research, Denmark. A pre-clinical scanner operating at 2.35 T (Bruker, Germany) located at Imagnia, Sweden was also used.

5.3. T_1 determination

T_1 measurements at thermal equilibrium were performed with the standard Inversion Recovery pulse sequence. The data were fitted to:

$$I = I_0\left[1 - A^* \exp(-t/T_1)\right] \quad (1)$$

T_1 measurements in a hyperpolarized state consisted of recording the decay curve of the hyperpolarized signal. The data were analyzed using the standard decay equation, where the effect of RF pulsation on the decay rate was neglected owing to the use of a small flip angle (3°). Curve fitting was carried out using the Matlab software (The MathWorks Inc., Natick, MA, USA).

5.4. Hyperpolarization

For the CMP2 hyperpolarization experiment, [1,1,2,2-D_4,2-^{13}C] choline chloride (27.3 mg, 189 µmol) was mixed with 7.1 mg of an aqueous solution of OX063 (61 mM) and ProHance (2.9 mM). The concentrations in the final DNP preparation were choline 6 M, OX063 14 mM and ProHance 0.7 mM. For the pyruvate hyperpolarization experiment, [1-^{13}C]pyruvic acid (120 mg, 1.34 mmol) was mixed with OX063 (1.9 mg, 1.3 µmol) and 2.1 µl of an aqueous solution of ProHance (30 mM). The final concentrations were OX063 14 mM and ProHance 0.7 mM. Samples for DNP were taken from these stock solutions.

The contrast agent ProHance was added to the preparations as it was previously shown that the addition of a Gd complex to the solid-state preparation increases the polarization level reached at 3.35 T (37). The DNP samples were hyperpolarized in a 3.35 T home-built dissolution DNP polarizer at ca. 1.3 K, 93.9 GHz and 100 mW.

5.5. Dissolution

Dissolution of CMP2 was performed with 4 ml of 40 mM phosphate buffer (pH 7.3) containing 100 mg/l EDTA. The sample was collected directly into a 10 mm NMR tube with a final [1,1,2,2-D_4,2-^{13}C]choline chloride concentration ranging between 20 and 46 mM. Dissolution of pyruvate was performed with 4 ml of 40 mM phosphate buffer (pH 7.3) containing 100 mg/l EDTA, with the addition of sodium hydroxide from a concentrated solution to compensate for the acid content. The transfer time was ca. 20 s, measured as the time between dissolution and the first pulse taken in the spectrometer.

5.6. Enhancement factor calculation

The calculation of the enhancement and percentage polarization in solution was performed by dividing the hyperpolarized signal (single scan, 5° pulse) by the thermal equilibrium signal of the same sample and considering that the thermal polarization according to the Boltzmann distribution at the specific field and temperature. For the thermal equilibrium measurement, 70 µl of Omniscan (0.5 M Gadolinum complex) was added to the sample to ensure the decay of the hyperpolarized state and to shorten the T_1 to allow for fast averaging. Owing to the low SNR of the sample at thermal equilibrium, this signal was averaged 512 times using the same acquisition parameters and a repetition time of 3.5 s. Signal averaging was accounted for in the enhancement factor calculation.

5.7. Studies in whole blood

A 4 ml aliquot of human blood was drawn from a single healthy subject into a heparinized tube. A 2.8 ml aliquot of the blood

was transferred to a 10 mm NMR tube. Next, 300 µl of hyperpolarized media were added to the tube, it was gently mixed and quickly placed in a 14.1 T spectrometer. A decay curve was recorded from a series of 5° pulses with a delay of 3 s in between.

5.8. Synthesis of [1,1,2,2-D_4, 2-^{13}C]acetylcholine

Forty units of carnitine acetyltransferase were dissolved in 60 mM TRIS buffer containing 5 mM Acetyl CoA in a 5 mm NMR tube. [1,1,2,2-D_4, 2-^{13}C]choline chloride (5 mM) was added to the reaction mixture, and the tube was gently mixed and left overnight at 37 °C. A mixture of [1,1,2,2-D_4, 2-^{13}C]choline and [1,1,2,2-D_4, 2-^{13}C]acetylcholine was expected as this enzyme is known to catalyze an equilibrium between L-carnitine and acetyl-L-carnitine.

5.9. Declaration of interest

Rachel Katz-Brull is an employee and shareholder of BrainWatch Ltd. Hyla Allouche-Arnon is an employee of BrainWatch Ltd. Mathilde Lerche and Magnus Karlsson are employees and shareholders of Albeda Research.

Acknowledgments

We thank Elena Vinogradov for discussions on deuterium decoupling. We thank Tali Scherf for assistance with the implementation of deuterium decoupling. This study has been supported in part by the DANA foundation, the Bi-National Science Foundation (BSF, grant number 2006118), the German Israel Foundation (GIF, grant number 2131–1586.5/2006), the Abisch-Frenkel Foundation, the Center for Complexity Science (grant number GR2007-053) and BrainWatch Ltd. R.K.B. is thankful for the generosity of the Tchorz Fund, the Speijer Inheritance Fund and the Goldin–Savad Inheritance Fund.

REFERENCES

[1] Ardenkjaer-Larsen JH, Fridlund B, Gram A, Hansson G, Hansson L, Lerche MH, Servin R, Thaning M, Golman K. Increase in signal-to-noise ratio of >10,000 times in liquid-state NMR. Proc Natl Acad Sci USA 2003; 100(18): 10158–10163.
[2] Golman K, in 't Zandt R, Thaning M. Real-time metabolic imaging. Proc Natl Acad Sci USA 2006; 103(30): 11270–11275.
[3] Gallagher FA, Kettunen MI, Hu DE, Jensen PR, in't Zandt R, Karlsson M, Gisselsson A, Nelson SK, Witney TH, Bohndiek SE, Hansson G, Peitersen T, Lerche MH, Brindle KM. Production of hyperpolarized [1,4-C-13(2)]malate from [1,4-C-13(2)]fumarate is a marker of cell necrosis and treatment response in tumors. Proc Natl Acad Sci USA 2009; 106(47): 19801–19806.
[4] Grant AK, Vinogradov E, Wang X, Lenkinski RE, Alsop DC. Perfusion imaging with a freely diffusible hyperpolarized contrast agent. Magn Reson Med 2011; doi: 10.1002/mrm.22860.
[5] Mishkovsky M, Comment A, Gruetter R. In vivo detection of rat brain metabolism using hyperpolarized acetate. Proc Int Soc Mag Reson Med (Stockh) 2010; 18: 3278.
[6] Keshari KR, Wilson DM, Chen AP, Bok R, Larson PEZ, Hu S, Van Criekinge M, Macdonald JM, Vigneron DB, Kurhanewicz J. Hyperpolarized [2-^{13}C]-fructose: a hemiketal DNP substrate for in vivo metabolic imaging. J Am Chem Soc 2009; 131(48): 17591–17596.
[7] Wilson DM, Hurd RE, Keshari K, Van Criekinge M, Chen AP, Nelson SJ, Vigneron DB, Kurhanewicz J. Generation of hyperpolarized substrates by secondary labeling with [1,1-C-13] acetic anhydride. Proc Natl Acad Sci USA 2009; 106(14): 5503–5507.
[8] Karlsson M, Jensen PR, Zandt R, Gisselsson A, Hansson G, Duus JØ, Meier S, Lerche MH. Imaging of branched chain amino acid metabolism in tumors with hyperpolarized 13C ketoisocaproate. Int J Cancer 2009; 127(3): 729–736.
[9] Allouche-Arnon H, Gamliel A, Barzilay CM, Nalbandian R, Gomori JM, Karlsson M, Lerche MH, Katz-Brull R. A hyperpolarized choline molecular probe for monitoring acetylcholine synthesis. Contrast Media Mol Imag 2011; 6(1): doi:10.1002/cmmi.418.
[10] Katz-Brull R, Koudinov AR, Degani H. Direct detection of brain acetylcholine synthesis by magnetic resonance spectroscopy. Brain Res 2005; 1048(1–2): 202–210.
[11] Moreno KX, Sabelhaus SM, Merritt ME, Sherry AD, Malloy CR. Competition of pyruvate with physiological substrates for oxidation by the heart: implications for studies with hyperpolarized [1-C-13] pyruvate. Am J Physiol Heart C 2010; 298(5): H1556–H1563.
[12] Harris T, Eliyahu G, Frydman L, Degani H. Kinetics of hyperpolarized C-13(1)-pyruvate transport and metabolism in living human breast cancer cells. Proc Natl Acad Sci USA 2009; 106(43): 18131–18136.
[13] Gabellieri C, Reynolds S, Lavie A, Payne GS, Leach MO, Eykyn TR. Therapeutic target metabolism observed using hyperpolarized N-15 choline. J Am Chem Soc 2008; 130(14): 4598–4599.
[14] Kurhanewicz J, Vigneron DB, Brindle K, Chekmenev EY, Comment A, Cunningham CH, DeBerardinis RJ, Green GG, Leach MO, Rajan SS, Rizi RR, Ross BD, Warren WS, Malloy CR. Analysis of cancer metabolism by imaging hyperpolarized nuclei: prospects for translation to clinical research. Neoplasia 2011; 13(2): 81–97.
[15] Albers MJ, Bok R, Chen AP, Cunningham CH, Zierhut ML, Zhang VY, Kohler SJ, Tropp J, Hurd RE, Yen Y-F, Nelson SJ, Vigneron DB, Kurhanewicz J. Hyperpolarized ^{13}C lactate, pyruvate, and alanine: noninvasive biomarkers for prostate cancer detection and grading. Cancer Res 2008; 68: 8607–8615.
[16] Chen AP, Tropp J, Hurd RE, Van Criekinge M, Carvajal LG, Xu D, Kurhanewicz J, Vigneron DB. In vivo hyperpolarized C-13 MR spectroscopic imaging with H-1 decoupling. J Magn Reson 2009; 197(1): 100–106.
[17] Akasaka K, Imoto T, Shibata S, Hatano H. Deuterium substitution effect on relaxation times (Desert) and its application to study of conformation of some purine nucleoside derivatives. J Magn Res 1975; 18(2): 328–343.
[18] Maltseva TV, Foldesi A, Chattopadhyaya J. T_1 and T_2 relaxations of the C-13 nuclei of deuterium-labeled nucleosides. Magn Res Chem 1998; 36(4): 227–239.
[19] Chekmenev EY, Hovener J, Norton VA, Harris K, Batchelder LS, Bhattacharya P, Ross BD, Weitekamp DP. PASADENA hyperpolarization of succinic acid for MRI and NMR spectroscopy. J Am Chem Soc 2008; 130(13): 4212.
[20] Hovener JB, Chekmenev EY, Harris KC, Perman WH, Robertson LW, Ross BD, Bhattacharya P. PASADENA hyperpolarization of C-13 biomolecules: equipment design and installation. Magnet Reson Mater Phys Biol Med 2009; 22(2): 111–121.
[21] Hovener JB, Chekmenev EY, Harris KC, Perman WH, Tran TT, Ross BD, Bhattacharya P. Quality assurance of PASADENA hyperpolarization for C-13 biomolecules. Magn Reson Mater Phys Biol Med 2009; 22(2): 123–134.
[22] Blusztajn JK. Choline, a vital amine. Science 1998; 281(5378): 794–795.
[23] Kohler SJ, Yen Y, Wolber J, Chen AP, Albers MJ, Bok R, Zhang V, Tropp J, Nelson S, Vigneron DB, Kurhanewicz J, Hurd RE. In vivo (13) carbon metabolic imaging at 3 T with hyperpolarized C-13-1-pyruvate. Magn Reson Med 2007; 58(1): 65–69.
[24] Cudalbu C, Comment A, Kurdzesau F, van Heeswijk RB, Uffmann K, Jannin S, Denisov V, Kirik D, Gruetter R. Feasibility of in vivo N-15 MRS detection of hyperpolarized N-15 labeled choline in rats. Phys Chem Chem Phys 2010; 12(22): 5818–5823.
[25] Sarkar R, Comment A, Vasos PR, Jannin S, Gruetter R, Bodenhausen G, Hall H, Kirik D, Denisov VP. Proton NMR of (15)N-choline metabolites enhanced by dynamic nuclear polarization. J Am Chem Soc 2009; 131(44): 16014–16015.
[26] Romijn JA, Chinkes DL, Schwarz JM, Wolfe RR. Lactate–pyruvate interconversion in blood – implications for in-vivo tracer studies. Am J Physiol 1994; 266(3): E334–E340.
[27] Day SE, Kettunen MI, Gallagher FA, Hu DE, Lerche M, Wolber J, Golman K, Ardenkjaer-Larsen JH, Brindle KM. Detecting tumor response to treatment using hyperpolarized ^{13}C magnetic resonance imaging and spectroscopy. Nat Med 2007; 13(11): 1382–1387.
[28] Allen DD, Smith QR. Characterization of the blood–brain barrier choline transporter using the in situ rat brain perfusion technique. J Neurochem 2001; 76(4): 1032–1041.

[29] Grunewald RW, Oppermann M, Muller GA. Choline transport and its osmotic regulation in renal cells derived from the rabbit outer medullary thick ascending limb of Henle. Pflug Arch Eur J Phys 1997; 434(6): 815–821.
[30] Moseley RH, Takeda H, Zugger LJ. Choline transport in rat liver basolateral plasma membrane vesicles. Hepatology 1996; 24(1): 192–197.
[31] Antai AB, Eyong EU, Eteng MU, Itam EH, Eko ME, Ita SO. Serum protein and enzyme levels in rats following administration of ethanolic leaf extract of Ageratum conyzoides (goat weed). Niger J Physiol Sci 2009; 24(2): 117–120.
[32] Katz-Brull R, Seger D, Rivenson-Segal D, Rushkin E, Degani H. Metabolic markers of breast cancer: enhanced choline metabolism and reduced choline–ether phospholipid synthesis. Cancer Res 2002; 62(7): 1966–1970.
[33] Muller SA, Holzapfel K, Seidl C, Treiber U, Krause BJ, Senekowitsch-Schmidtke R. Characterization of choline uptake in prostate cancer cells following bicalutamide and docetaxel treatment. Eur J Nucl Med Mol Imag 2009; 36(9): 1434–1442.
[34] Horoszewicz JS, Leong SS, Kawinski E, Karr JP, Rosenthal H, Chu TM, Mirand EA, Murphy GP. Lncap model of human prostatic carcinoma. Cancer Res 1983; 43(4): 1809–1818.
[35] Plathow C, Weber WA. Tumor cell metabolism imaging. J Nucl Med 2008; 49: 43–63.
[36] Fowler JS, Logan J, Wang GJ, Volkow ND, Telang F, Ding YS, Shea C, Garza V, Xu Y, Li Z, Alexoff D, Vaska P, Ferrieri R, Schlyer D, Zhu W, John Gatley S. Comparison of the binding of the irreversible monoamine oxidase tracers, [(11)C]clorgyline and [(11)C]l-deprenyl in brain and peripheral organs in humans. Nucl Med Biol 2004; 31(3): 313–319.
[37] Ardenkjaer-Larsen JH, Macholl S, Johannesson H. Dynamic nuclear polarization with trityls at 1.2 K. Appl Magn Reson 2008; 34(3–4): 509–522.